Published in final edited form as:
Lab Invest. 2009 November ; 89(11): 1317–1328. doi:10.1038/labinvest.2009.94.

Paracrine Induction of Endothelium by Tumor Exosomes

Joshua L. Hood, **Hua Pan**, **Gregory M. Lanza**, and **Samuel A. Wickline**
Consortium for Translational Research In Advanced Imaging and Nanomedicine (C-TRAIN), Washington University School of Medicine, 4320 Forest Park Avenue, Suite 101, Campus Box 8215, St. Louis, MO 63108

Joshua L. Hood: jhood@path.wustl.edu; Hua Pan: hpan@cmrl.wustl.edu; Gregory M. Lanza: greg.lanza@mac.com; Samuel A. Wickline: WICKLINES@aol.com

Abstract

Cancers utilize a nanoscale messenger system known as exosomes to communicate with surrounding tissues and immune cells. However, the functional relationship between tumor exosomes, endothelial signaling, angiogenesis, and metastasis is poorly understood. Herein, we describe a standardized approach for defining the angiogenic potential of isolated exosomes. We created a powerful technique to rapidly and efficiently isolate and track exosomes for study using dynamic light scattering in conjunction with fluorescent exosome labeling. With these methods, melanoma exosomes were observed to interact with and influence endothelial tubule morphology as well as move between endothelial tubule cells by means of tunneling nanotube structures. Melanoma exosomes also were observed to rapidly stimulate the production of endothelial spheroids and endothelial sprouts in a dose-dependent manner. In concert, tumor exosomes simultaneously elicited paracrine endothelial signaling by regulation of certain inflammatory cytokines. These data suggest that, tumor exosomes can promote endothelial angiogenic responses, which could contribute to tumor metastatic potential.

Keywords

exosomes; angiogenesis; tumor; cancer; endothelial; 3D assay; cytokines

Cancer cells manipulate their microenvironment to optimize conditions for growth and metastasis in multiple ways. Recent evidence has suggested a novel mechanism for achieving this goal through the production and secretion of nanoscale membrane fragments known as tumor exosomes.(1) Exosomes are naturally occurring biological nanoparticles 30–100 nm in size (2–4). They are formed by the inward budding of multivesicular bodies (MVBs), a component of the endocytic pathway. Exosomes are constitutively generated and released into the surrounding extracellular matrix and circulation via fusion of MVBs with the plasma membrane. The nanoscale size of exosomes facilitates their penetration and interaction with host sites and cell types that are distant from an advancing tumor cell front and they have been shown to participate in cell to cell communication such as morphogen and RNA transport between cells (3). These transport processes can influence invasion of tumor cells, stimulate antigenic T-cell responses, modulate cell polarity and have a role in the developmental patterning of tissues (3). Exosomes also may play an important role in tumor immune evasion by direct suppression of immune cell activation (5), (6), (7).

Corresponding Author: Samuel A. Wickline M.D., Phone: 314-454-8635, WICKLINES@aol.com, Fax: 314-454-5265.
Reprint Request: Samuel Wickline, (WICKLINES@aol.com), 320 Forest Park Ave., Suite 101, Campus Box 8215, St. Louis MO 63108

In order to metastasize to distant sites, tumor cells typically require a "prepared environment" to establish successful implantation and growth (8). One model suggests that metastatic cells cooperate in waves (8). Early waves of metastatic cells prepare distal sites for interactions with subsequent waves to form metastatic foci. Additionally, reactive lymph nodes that are downstream of tumors undergo lymphangiogenesis in preparation for tumor metastasis (9). Knowledge of how such sites are induced to become receptive to tumor implantation remains incomplete; although, in the case of melanoma, upstream secretion of soluble angiogenic signaling molecules such as VEGF play a role (9), (10). Regardless of the mechanism, it would seem necessary that cancers such as melanoma would be capable of signaling site preparation for eventual metastasis. Moreover, little is known about the role of melanoma exosomes in angiogenesis. We hypothesize that melanoma exosomes might serve as nanocarriers of paracrine effectors of endothelium to prepare distal sites for docking of metastatic cells.

To elucidate the role of melanoma exosomes as nanovehicles that might pave the way for tumor cell implantation, we developed and validated a new *in vitro* 3D angiogenesis assay system that incorporates a continuum of both tubulogenesis (early endothelial angiogenic changes) and spheroid sprouting (later endothelial angiogenic changes) to test exosomes derived from experimental tumor cell lines. The system also incorporates a new exosome labeling, isolation and tracking approach using stable fluorescent carbocyanine dyes. The rationale for establishing a new screening approach stems in part from the technical challenges of dealing with the exosome constructs themselves, which are very difficult to isolate and apply in large quantities even *in vitro*, much less *in vivo* in tissue angiogenesis studies. Because exosomal constituents and activities are likely to change over time as the tumor cell itself adapts to local environments and the selective pressure of therapeutics, a rapid assay of *in vitro* activity of patient-derived exosomes could be invaluable for clinical therapeutic decision making. An *in vitro* assay also would allow conjunctive readouts such as cytokine or RNA microarray analyses of sprouting endothelial cells.

We show for the first time that melanoma exosomes can be successfully labeled, isolated and tracked using fluorescent carbocyanine dyes. Tracking of melanoma exosomes within endothelial cell cultures reveals a novel association between exosomes and cellular nanotubes. Moreover, the endothelial response to melanoma exosomes is a complicated phenomenon that exhibits both trophic and proliferative changes in a dose dependent manner which simultaneously modulates both angiogenic and immunologic cytokine signaling. The implication is that the melanoma "exosomal messenger system" is capable of multifunctional paracrine bioactivities that facilitate tumor communication at a distance, especially in the matter of turf preparation, which could be assessed *in vitro* in individual tumor types from single sources.

MATERIALS AND METHODS

Materials and cell culture

The 2F-2B mouse endothelial cell line was purchased from ATCC (CRL-2168) and maintained in 2D culture with Dulbecco's modified Eagle's medium with 4.5 g/L glucose, 90%; heat-inactivated fetal bovine serum, 10% at 37°C and 5% CO_2. 2F-2B cells were cultured with EGM-2 media (Clonetics catalog CC-3162) for 3D spheroid assays. Mouse B16-F10 melanoma cells were purchased from ATCC and maintained in culture with 90% DMEM and 10% heat inactivated fetal bovine serum at 37°C and 5% CO_2.

Isolation of exosomes

B16-F10 melanoma cell cultures were grown to 70% confluence in three 300 cm^2 flask. Culture media was removed and cells washed in PBS. Cells were cultured for 48 hrs in the presence of conditioned media. Conditioned culture media was prepared by subjecting normal culture media to overnight ultracentrifugation at 110,000 × g to remove bovine exosomes (11). B16 melanoma exosomes were collected from 48 hr culture in conditioned media through standard differential centrifugation steps using a 70 Ti rotor (11). Culture media was spun and supernatants collected from 300 × g for 10 min, 2000 × g for 10 min, to remove residual cells and debris, 10,000 × g for 30 min to remove microparticles (12), and 100,000 × g for 2 h (in the presence or absence of 1.0 μM DiI or DiR (InVitrogen, CA)). Exosome pellets were washed three times in PBS, pooled, and re-isolated in PBS at 100,000 × g for 2 hr. Exosome pellets were resuspended in 1 ml of PBS, protein content measured via BCA absorbance (Pierce) and stored at −80°C until use.

Flotation of exosomes on a continuous sucrose gradient

Flotation of exosomes on a continuous sucrose gradient (2.0 - 0.25 M sucrose, 20 mM HEPES/NaOH, pH 7.4) was performed similarly as previously described but using an SW 41 rotor (13). The gradient (prepared using a Hoefer, Inc. gradient maker) was spun for >15 hours at 100,000g and eleven 1 ml fractions were collected from the bottom up. The density of each fraction was calculated using a refractometer (11). 50 ul of each fraction was added to a black 96 well plate and DiR exosome fluorescence detected using a Xenogen IVIS fluorescent imager (Caliper Life Sciences). Each of the remaining fractions was resuspended in 24 ml of PBS and re-centrifuged for 1 hour at 110,000g to pellet exosomes. The protein level of each fraction was measured via BCA absorbance (Pierce) and exosome pellet diluted in Laemmli's sample buffer and run on a 4–20% Tris-glycine gel (Biorad). Exosomal proteins were detected by western blot using anti-Melan A antibody (Santa Cruz biotechnology) and anti-Calnexin (Millipore).

Electron Microscopy

Purified exosome pellets were fixed with 2.5% gluturaldehyde in PBS for 30 minutes on ice. After rinsing, the pellet was sequentially stained with osmium tetroxide and uranyl acetate; then dehydrated and embedded in Polybed 812. Tissue was thin sectioned on a Reichert-Jung Ultracut, viewed on a Zeiss 902 Electron Microscope, and recorded with Kodak E.M. film. E.M. reagents were purchased from Electron Microscopy Sciences.

Fumagillin nanoparticle formulation

Perfluorocarbon nanoparticles were prepared as described previously (14), (15). Briefly, the emulsions comprised 20% (vol/vol) perfluoro-15-crown-5 (Exfluor Research Corporation), 2% (wt/vol) of a surfactant comixture, 1.7% (wt/vol) glycerin, and water for the balance. The surfactant comixture included 98 mole% lecithin (Avanti Polar Lipids Inc), 1.8 mole% phosphatidylethanolamine (Avanti Polar Lipids Inc), and in chloroform:methanol (3:1), which was dried to a lipid film under vacuum. Nanoparticle formulations included 0.2 mole % fumagillin (a gift from the National Cancer Institute), which was added to the surfactant mixture at the proportionate expense of lecithin. The surfactant components were prepared as published (14),(15) combined with PFOB and distilled deionized water, and emulsified (Microfluidics Inc) at 20,000 psi for 4 minutes. Particle sizes were determined at 37°C with a laser light scattering submicron particle analyzer (Brookhaven Instruments Corp.).

Spheroid angiogenesis assay

2F-2B cells were cultured 2-dimensionally in 75 cm^2 culture flask, isolated and applied to the wells of a 48 well (Corning) culture plate (50,000 cells/well) containing 200 μL of

prepared 1x matrigel (BD Biosciences) per well and 1 ml of EGM-2 culture media. When used, 2F-2B or B16 melanoma exosomes were applied to the endothelial culture wells at 0, 2.5, 5 or 10 μg/ml protein concentrations. Spheroids were allowed to develop at 37°C and 5% CO2 and were observed via phase contrast microscopy using a Nikon Diaphot 300 microscope and images recorded using a Basler A302fc microscope camera in conjunction with Vision Assist software for the number and size of spheroids as well as the presence or absence of endothelial sprouts. Sizes and numbers of spheroids were computed in randomly selected high powered fields of view by ImageJ analysis software (Rasband, W.S., ImageJ, U. S. National Institutes of Health, Bethesda, Maryland, USA, http://rsb.info.nih.gov/ij/, 1997–2008).

Fluorescent and Confocal Microscopy

2F-2B endothelial cells (100,000 cells/chamber) were cultured on matrigel (200 ul), in the presence or absence of 20 μg/ml of fluorescent red DiI (1,1′-dioctadecyl-3,3,3′3′-tetramethylindocarbocyanine perchlorate) labeled (1μM) 2F-2B or B16 melanoma exosomes for 24 hrs, coating the bottom of a 4 chamber microscopy culture slide (LabTek). After 24 hrs of incubation, endothelial tubules were fixed for 10 min. with 3.7% paraformaldehyde, washed 3X with PBS, and extracted with acetone at −20 C for 5 min and blocked with 1% BSA in PBS for 30 min. Tubules were then washed 3X with PBS and stained with AlexaFluor 488 phalloidin according to manufacturer's protocol (invitrogen). Briefly, 2 units of methanolic stock solution was diluted into 200 ul of PBS containing 1% BSA and added to each slide chamber containing tubules to stain actin cytoskeleton green for 20 minutes at room temp. Chamber slides were then washed 3X with PBS and sealed with DAPI (stains nuclei fluorescent blue) VECTASHIELD mounting media (Vector Labs, CA). Slides were then visualized using an Olympus BX61 fluorescent or confocal (Zeiss Meta 510, Thornwood, NY) microscope using standard filter sets.

Cytokine array analysis

2F-2B endothelial cells were cultured for 72 hrs to form spheroids followed by the addition of 0, 2.5, or 10 μg/ml B16 melanoma exosomes for 10 days to produce cytokines in the spheroid culture media. Three sets of culture media samples were collected and pooled for each exosome dosing group and analyzed using two different cytokine arrays: 1. TransSignal Mouse Angiogenesis array; (Panomics, Fremont CA) and 2. Mouse Proteome Profiler array (R&D Systems; Minneapolis MN) following the manufacturer's instructions provided with the kits. Fluorescent signals were processed using Kodak BioMax light radiographic film for Streptavidin-HRP based chemiluminescent detection. Film results were scanned and digitized using an Hewlett Packard Scanjet 3970 flatbed scanner. Individual cytokine signal intensities were evaluated using ImageJ analysis software (Rasband, W.S., ImageJ, U. S. National Institutes of Health, Bethesda, Maryland, USA, http://rsb.info.nih.gov/ij/, 1997–2008). Results are reported as average cytokine signal intensity based on pixel density.

Statistics

For spheroid sizing and cell proliferation, ANOVA was used to calculate statistical significance $p < 0.05$ between exosome treatment and control groups. For cytokine array analysis, the absolute value of the average percentage change (avg. of 2.5 and 10 μg/ml) over normalized control (0 μg/ml of exosomes) was calculated for each cytokine. Cytokine levels that changed more than 10% from the absolute value average changes as compared to a normalized control group were considered to be affected by the experimental procedures, according to ANOVA that revealed statistical significance ($p < 0.05$) for difference from control in each case.

RESULTS

Development of an endothelial spheroid assay for exosomal activation

The methods and assay system described herein recognize prior work by Haspel et al. (16) and Stahl et al. (17), but the present approaches exploit a newly discovered natural tendency of readily available standard cell types (2F-2B endothelial cells from ATCC) to spontaneously aggregate on matrigel to form 3D endothelial spheroids. These cells are derived from an SV40 transformed cell line originally generated for anti-angiogenic pharmacology studies (18). The cell line expresses common endothelial markers as well as endothelial markers present on B16 melanoma and human tumor vasculature making it ideally suited for angiogenic studies.

2F-2B mouse endothelial cell spheroids were created by culturing cells on matrigel. Surprisingly, 2F-2B cells exhibited a rare ability to spontaneously aggregate into uniformly distributed spheroids (Fig. 1a) when placed on matrigel in contrast to other cell types, such as SMHEC4 endothelial cells, which require prolonged artificial pre-formation in round bottom 96 well plates to induce spheroid formation (16). The individual 2F-2B endothelial cells migrate toward each other forming a lace-like network by 4 hrs. By 24 hrs the cells have aggregated into thick tubules in the process of contracting into spheroids. By 72 hrs, tubules have fully contracted leading to the formation of round spheroids. Looking ahead to 7 days, spheroids develop numerous “capillary-like” sprouts around their circumference. Some of the sprouts from adjacent spheroids will form anastomotic junctions of communication (Fig. 1b).

Having successfully generated endothelial spheroids, we next sought to assess whether they respond to a potent anti-angiogenic compound by growing the spheroids in the presence of fumagillin. Fumagillin is a mycotoxin produced by *aspergillus fumigatus* (14), (15) and is a potent inhibitor of angiogenesis operating by targeting the methionine aminopeptidase-2 of endothelial cells (19). We have previously shown that fumagillin itself, which is hydrophobic, can be incorporated into the lipid shell of a perfluorocarbon-core nanoparticle to overcome its poor solubility in aqueous solutions and allow for concentrated delivery to angiogenic blood vessels that form in various pathologies, resulting in their marked suppression (14), (15). Thus, when 2F-2B cells were treated with antiangiogenic fumagillin nanoparticles for 72 hrs, spheroids do not form in 3D cultures, which validate the proposed assay for assessing angiogenesis induction (Fig. 1c).

Methods for isolation of tumor exosomes *in vitro*

Based on current methodology, exosomes can be differentiated from other membrane particulate matter according to three criteria: 1.) size (~30–100 nm), 2.) unique flotation density (1.22-1.08 g/ml) on continuous sucrose gradients (13),(12),(20),(21),(22),(11) and 3.) characteristic “cup shaped” morphology via electron microscopy versus black “electron dense” microparticles (20). Mouse B16 melanoma cells were cultured and exosomes isolated by differential centrifugation (Fig. 2)(11). Although the standard approach for verification of exosome isolation relies on electron microscopy,(11) dynamic light scattering (Brookhaven Instruments Corp.) was used to size B16 melanoma exosomes (74 +/− 13 nm) (Fig. 2a) just prior to exosome pelleting at 100,000g (Fig. 2b). We find that sizing exosomes after pellet formation results in erroneous results given the tendency for exosomes to clump. The measurement can be performed conveniently in as little as 10 minutes, and greatly expedites confirmation of exosome isolation over traditional electron microscopy techniques (Fig. 2d). Exosomes were pelleted (Fig. 2b) at 100,000g for 2 h in the presence of DiI or DiR (1 μM) to fluorescently label exosomes (DiI used in Fig. 2b and DiR used in Fig. 2c). DiI (1,1′-dioctadecyl-3,3,3′3′-tetramethylindocarbocyanine perchlorate) or DiR (1,1′-

dioctadecyl-3,3,3′,3′-tetramethylindotricarbocyanine iodide) are lipophilic fluorescent red (DiI) or infrared (DiR) carbocyanin dyes that remain stable for days in living cultures and exosomes and undergo negligible transfer between intact membranes (Invitrogen, CA) which allows it to remain associated with exosomes exclusively. To confirm the density of our B16 melanoma exosome population isolated by differential centrifugation, DiR labeled B16 exosomes were separated on a continuous sucrose gradient. Because melanoma exosomes contain very few of the standard exosomal protein markers (11), and exosome identification with markers may miss up to 50% of exosomes depending on the antibody used (12), we reasoned that tracking exosomes on sucrose gradients with DiR would expedite the process of determining exosome density. As shown, B16 melanoma exosomes isolated on a continuous sucrose gradient exhibit an exosome density between 1.10 – 1.21 g/ml (Fig. 2c). This exosome density has been confirmed by many laboratories to range from ~ 1.08 to 1.22 g/ml for a variety or exosome types (13), (12), (11), including melanoma exosomes (21), (22). Moreover, the position of the exosomes on the gradient directly corresponds to the protein content of the fractions. Finally, the B16 melanoma exosomes expressed one of the few unique melanoma exosomal markers (Melan A/MART-1) (23), (11) and did not express the contaminant endoplasmic reticulum marker calnexin (23).

Finally, we confirmed isolation of B16 melanoma exosomes morphologically (Fig. 2d) using electron microscopy. As shown, B16 exosomes isolated by differential centrifugation express the characteristic “cup shaped ” morphology associated with exosomes (20) and are ~ 50 –100 nm in diameter, confirming our analysis by dynamic light scattering. Thus, with the use of these techniques we confirm successful isolation of B16 melanoma exosomes at the correct size, density, and morphology reported for exosomes.

Tumor exosomes engage endothelial tubule networks in 3D

Having successfully isolated melanoma exosomes, the next aim was to determine whether they interact with and influence the morphology of endothelial vasculature in our 3D culture model. 2F-2B (control) endothelial exosomes (Fig 3b) and B16 melanoma exosomes (Fig 3c,d) were fluorescently labeled and incubated with 3D cultured 2F-2B endothelial cells for 24 hrs to compare their influence on endothelial tubule formation to non-exosome treated tubules (Fig. 3a). As shown in Figure 3, cell nuclei are stained with fluorescent blue DAPI (VECTASHIELD mounting media, Vector Labs, CA), the connecting tubule networks are visualized with fluorescent green staining of the actin cytoskeleton with AlexaFluor 488 phalloidin (Invitrogen, CA), and exosomes stained with DiI reveal tubule interactions.

We observed that exosomes interact with developing endothelial tubules in novel ways. Compared with controls (Fig 3a), melanoma exosomes (Fig 3c) alter the morphology of the tubule network in a manner that favors increased tubule branching, whereas 2F-2B exosomes (Fig 3b) appear to decrease tubule branching and connections. We conclude that exosomes readily interact with tubule membranes because exosome signal appears within the cell bodies that make up connecting tubules and the developing spheroid cytoplasm (Fig 3b,c). The location of the exosome signal does not coincide with the nucleus (Fig 3b,c). However, co-localization of exosomes with cytoskeleton is observed for melanoma exosomes (Fig 3c,d) but minimally with 2F-2B exosomes (Fig 3b). This suggests differential compartmentalization of melanoma compared to 2F-2B exosomes in the cell.

The fluorescent signal for tumor exosomes acting as paracrine effectors appears different than the autocrine signal of endothelial exosomes. Melanoma exosome signal (Fig 3c) is both continuous throughout the tubule network and found in clusters whereas endothelial exosome signal is found predominantly in clusters (Fig 3b). The clustering of exosomes at focal points within the tubule network (Fig 3b) suggests organization of the exosomes within organelle structures such as endosomes. The observation that melanoma exosome signal

colocalizes with f-actin and is present throughout anastomotic connections between adjoining cellular clusters supports the existence of a transport process for relaying exosomal messages between cells of the endothelial tubule network (Fig 3c). These data are consistent with the hypothesis that endothelial cells transport tumor exosomes between cells by way of tunneling nanotubule networks (TNTs) containing actin cytoskeleton (Fig 3d). TNT's were recently shown to transport HIV-1 particles, membrane vesicles and endosomal organelles between cells (24), (25), (26). This has important implications for how tumors communicate with and influence vasculature for propagation and survival.

Tumor exosomes induce dose dependent endothelial spheroid responses

Having demonstrated the ability of melanoma exosomes to interact with and promote endothelial tube formation over the course of 24 hrs, the next experiments sought to determine the long term effects of melanoma exosomes on spheroid development. It is known that exosomes can modulate tissue patterning (3), which is a permanent effect, and therefore we hypothesized that once exposed to melanoma exosomes, the endothelial cells would undergo a long term change as evidenced by their pattern of cytokine expression. Thus, endothelial spheroids were developed for 72 hrs followed by application of a one time dose of a range of exosome concentrations between 0 and 10 μg/ml for 10 days. It is important to note that we did not expect melanoma exosomes to be present in culture after 10 days following their initial application on day one. Instead, we were interested in the permanence of the changes induced by the melanoma exosomes over time. Spheroid morphology, number and proliferation was then assessed (Fig. 4). Distinct morphological differences are easily observed via microscopic visualization of representative spheroids by 13 days (Fig. 4a) and thus provide a visual way to coordinate timing for subsequent analyses such as spheroid proliferation or cytokine production. Long term culture of native 2F-2B spheroids (Fig. 4a) produced fine branching "needle-like" endothelial sprouts as seen on aortic ring models (27). However, in the presence of 2.5 μg/ml of melanoma exosomes, spheroid sprouts exhibited increased complexity in terms of size and number (Fig. 4a). Increasing the exosome concentration to 5 or 10 μg/ml resulted in suppressed formation of the larger spheroid bodies (excluding circumferential tubules) in favor of more numerous smaller ones (Fig. 4a,b) that manifested less endothelial sprouting (Fig. 4a) and quantitatively increased proliferation (Fig. 4c). This observed bimodal dose-dependent response to exosome stimulation indicates that spheroids exhibit *sprout enlargement* at lower concentrations; yet at higher exosome concentrations the *rate* of spheroid enlargement and sprouting is augmented with smaller more numerous spheroids.

These morphological data provide evidence to support the hypothesis that the differential response to tumor exosomes is attributable to *trophic signaling* at lower doses, but *proliferative signaling* (in less mature spheroids) at higher doses. Taken together, these data suggest that at lower concentrations melanoma exosomes could promote spheroid maturation and sprouting angiogenesis leading to anastomotic communication networks. At higher concentrations, melanoma exosomes may favor increased endothelial proliferation inducing smaller, more numerous, and less mature-appearing spheroids.

Cytokine signaling induced by exosomes

In view of the previously reported effect of tumor growth on down regulation of endothelial inflammatory biomarkers (e.g., vascular adhesion molecules) that may facilitate escape from immune surveillance (6), (7), and the established role of cytokines in tumor-endothelial cell communication (28), we sought to delineate the effect of melanoma exosomes on endothelial inflammatory cytokine production (29). Although melanoma exosomes induce a dose dependent bimodal influence on spheroid formation as shown by our assay (Fig. 4), we further hypothesized that exosomes might simultaneously suppress endothelial production of

pro-inflammatory cytokines. Accordingly, endothelial spheroids were developed for 72 hrs on matrigel followed by the addition of 0, 2.5 or 10 μg/ml of melanoma exosomes for 10 days. Spheroid culture supernatants were then collected and analyzed using angiogenic (Panomics mouse angiogenesis array; Fremont CA) (Fig. 5a) and inflammatory cytokine (mouse proteome profiler array (R&D Systems; Minneapolis MN) (Fig. 5b,c) arrays.

In general, we observed that the cytokine expression patterns could be subdivided into "concordant" (Fig. 5b) and "discordant" responses (Fig. 5a,c). Concordant cytokines are either unidirectionally increased (Fig. 5b) regardless of the exosome dosing, or undergo bidirectional regulation within the discordant groups (Fig. 5a,c). Overall, cytokines that might be considered pro-angiogenic increased with increasing exosome dosing: e.g., IL-1α, FGF, GCS-F, TNFα, Leptin, TGFα and VEGF (Fig. 5a). Interestingly, some inflammatory cytokines were suppressed at the higher exosome dose (Fig. 5c), which could mimic the situation *in vivo* when angiogenesis is stimulated in the face of reduced expression of vascular adhesion molecules (30). For example, reduced expression of the pro-inflammatory cytokines TREM-1 (31), I-TAC (32), IL-3 (33) and IL-16 (32) was observed at the 10 μg/ml dose of exosomes. Overall, these data provide supporting evidence for exosomal stimulation of endothelial angiogenic responses.

DISCUSSION

Angiogenesis is modulated not only by soluble angiogenic factors, but also by cell derived microparticles, microvesicles and exosomes. Important distinctions exist in the composition, analysis, and bioactivity, and use of these types of particles that require consideration when interpreting the present data. Microparticles comprise a heterogeneous population of particles 100–1000nm in dimension. They are formed by a regulated reverse budding mechanism where the plasma membrane blebs outward through reorganization of the underlying cortical actin cytoskeleton (34). This results in the direct detachment of plasma membrane buds into the extracellular space. Thus, microparticles represent one form of "shedding vesicle"(35). Microparticles can be separated from exosomes during differential centrifugation of cell culture supernatant between 10,000 to 14,000g (12),(33),(36).

Platelet microparticles (PMPs) and to a lesser extent endothelial microparticles (EMPs) are arguably the most studied shedding vesicles in large part a result of their pronounced role in mediating coagulation and thrombosis (37), (38), (39), (40). A number of studies have demonstrated a role for PMPs in promoting endothelial angiogenesis both *in vitro* and *in vivo* (41), (27), (42). In contrast, the influence of EMPs on angiogenesis has been mixed with some studies reporting increased endothelial tubulogenesis (36) or impaired endothelial proliferation and increased apoptosis (43) *in vitro*. Lymphocyte microparticles have also been shown to suppress angiogenesis *in vitro* and *in vivo* by interfering with VEGF signaling (44).

Microvesicles (microparticles + exosomes) derived from platelets (PMVs) induce VEGF mRNA expression in lung cancer cells and promote their adherence to endothelial cells (45). Microvesicles derived from cancer cells such as fibrosarcoma and prostate carcinoma (46), and ovarian carcinoma (47) also promote angiogenesis. Ovarian cancer microvesicles have been reported to carry VEGF (48). Glioblastoma microvesicles promote endothelial proliferation *in vitro* (49). In contrast to what is known about microparticle and microvesicle (microparticle + exosome) mediated angiogenic effects, much less is known about tumor exosome mediated angiogenesis alone. One report demonstrates intercellular transfer of a truncated form of epidermal growth factor receptor (EGFRvIII) from an EGFRvIII expressing cell line to a non-EGFRvIII expressing cell line via exosomes (50). Since VEGF gene expression is regulated by EGFRvIII, such receptor transfer may contribute to

angiogenic signaling on tumor cell subsets. Additionally, exosomes derived from a D6.1A tetraspanin transfected pancreatic cancer cell line promote D6.1A mediated endothelial tubulogenesis (51).

In our investigations, we have created a powerful and efficient technique using dynamic light scattering in conjunction with fluorescent labeling to rapidly and efficiently isolate and track exosomes. This methodology can be easily adapted to a variety of *in vitro* and *in vivo* exosome studies. Dynamic light scattering provides for rapid and accurate exosome sizing during purification steps. In contrast to standard confirmation of exosome isolation by electron microscopy, it is less time consuming (minutes versus days), not as technically challenging and does not result in any sample loss. This is very important for small volumes of human fluid samples where one cannot afford to spare exosomes to confirm their isolation.

Labeling exosomes with fluorescent carbocyanine dyes prior to separation on sucrose gradients allows for distinct exosome subpopulations present in a variety of culture or body fluids to be efficiently separated from one another without exploring for markers which may fluctuate on given populations depending on signaling or evolving pathological conditions or be lacking in specific exosome subsets. Such is the case with the platelet exosome marker CD63. CD63 can be used to distinguish platelet derived exosomes from platelet microparticles (PMPs) (12). However, CD63 is only expressed on ~ 50% of platelet exosomes making it possible to overlook non-CD63 bearing exosomes during exosome isolation. Our technique would not miss non-CD63 bearing exosomes and may discover unknown subsets.

Historically, the first use of sucrose gradient preparations of exosomes by Raposo et. al. was to determine whether MHC II proteins were bound to exosomes (13). It is important to note that they determined their exosome pellet, isolated by differential centrifugation, to be free of plasma membrane contaminants prior to flotation on a sucrose gradient (13). Regardless, their method established exosome density a criteria for confirming exosome isolation. Isolation of exosomes by flotation density on continuous sucrose gradients has since been confirmed by many groups and is very consistent ranging from ~ 1.08 to 1.22 g/ml for a variety or exosome types (13), (12), (11), including melanoma exosomes (21), (22).

We expanded on the original approach of Raposo et al. by tracking fluorescent labeled exosomes on continuous sucrose gradients, and confirmed that B16 melanoma exosomes isolated by differential centrifugation are in fact a relatively pure population of exosomes as confirmed by their presence at a density between 1.21 and 1.10 g/ml (fractions 4–6) (Fig. 2c). Moreover, the B16 melanoma exosomes were found to express one of the few unique melanoma exosomal markers (Melan A/MART-1) (23), (11) and do not express the endoplasmic reticulum contaminant marker calnexin (23). This technique is useful for processing small volumes of *in vivo* derived human fluid samples for functional exosomes studies or potential therapeutic applications where one cannot afford to spare exosomes to confirm their isolation via biomarkers. This further supports the high level of purity of B16 melanoma exosomes isolated by differential centrifugation and strongly validates our novel technique for fluorescently labeling, tracking and confirming exosome isolation through gradient centrifugation.

Additionally, we report for the first time the association of exosomes with cellular nanotube structures. This may have important implications for how normal or tumor derived exosomes interact with and transfer their messages between cells. We also report a dramatic action of native (unmodified) melanoma exosomes on endothelial regulation as evidenced by spheroid growth and the formation of early vasculature precursors such as endothelial

sprouts. A dose dependency was observed that implies a bimodal dose dependent trophic versus proliferative influence of melanoma exosomes that could have implications for further understanding fundamental mechanisms of the metastasis that accompany the tumor "angiogenic switch" as described originally by Hanahan and Folkman (52). These data suggest that melanoma cells may be capable of effecting angiogenesis from a distance through a membrane messenger (exosomal) system in the absence of direct cell to cell contact with endothelial cells. Our data indicate that no exogenous driver of angiogenesis is required under these experimental conditions, and that native melanoma exosomes already are capable of these actions.

Our data further suggest that tumor cells might communicate with and possibly control normal cells and tissues at sites distal from the tumor using exosomal paracrine effects to manipulate cytokine expression profiles. The possibility of an indirect mechanism of exosome-mediated immunosuppression would be potentiated by the known direct role of tumor exosomes in suppression of tumor cells (6), (53). Past studies have demonstrated exosome mediated immunosuppression of NK cells (6), apoptosis of anti-tumor T-cells, induction of myeloid suppressor cells and impairment of monocyte differentiation into tumor antigen presenting dendritic cells (7). In view of the likelihood that the concentration of tumor exosomes should be greatest nearest the tumor, the immune damping effect might be expected to increase as anti-tumor cells move closer to the actual tumor site.

Although this *in vitro* angiogenesis assay system cannot fully represent the complex *in vivo* situation, it is known that the morphological and physiological behavior of cells cultured in 2D differs considerably from that of fully spatial 3D pathology *in vivo*. Consequently, over the last few years a welcome shift toward development of fast and reliable 3D culture assay systems has emerged (54), (55), (56). These systems, while not a replacement for ultimately confirming findings *in vivo*, encompass the ease and reproducibility of 2D reductionist systems while better mimicking natural *in vivo* 3D tissue morphology. Only a few 3D angiogenesis model systems are available at present, but they require the purchase of expensive commercial kits (16), (57). Many commercial kits contain no source cell standardization that would ensure reproducibility.

In this assay, spontaneous aggregation of 2F-2B cells obviates the time consuming and tedious step of forcing endothelial spheroid formation via week long culture in round bottom 96 well plates (16), or 2 day culture on microcarriers (58). The assay offers multilevel angiogenic analyses for assessing differentiation of endothelial cells into higher order angiogenic structures. For example, the assay (Fig. 1) allows quantification of: 1) 3D migration of endothelial cells, 2) formation of endothelial tubules, 3) contraction of endothelial tubules into early spheroids, 4) formation of sprouting spheroids, 5) anastomosis of sprouts into capillary-like networks. Moreover, the evolution of these structures occurs unforced with a natural spontaneity within manageable points of time so that they can be studied independently of one another with the use of simple microscopic interrogation.

Although we only tested one type of tumor exosome from melanoma cells, the assay paradigm should serve as a test bed for other types as well. It may be the case that not all exosomes would elicit endothelial proliferation, but this might be important to determine *in vitro* before launching a campaign of anti-angiogenic therapy for example. It is also not established from these data exactly what is the stimulatory component of the exosome: the exosome itself, or effector molecules carried within. Clearly, an in depth analysis of B16 melanoma contents (protein, RNA etc.) will be necessary to explain the mechanism of our observations. The small amount of literature available for cancer patients suggest background, "normal" exosome concentrations well below that of circulating tumor exosomes (59). Healthy age matched control patients have negligible quantities of exosomes

in the circulation while exosome levels progressively increase with cancer stage, indicating the likely dependence of these responses on tumor specific exosomes. Further research will be required to tease out the nature of angiogenic exosome effectors, although exosomes are known to be replete with myriad potential candidates such as microRNA (59). Additionally, other secreted vesicles, glioblastoma microvesicles, have been shown to stimulate the proliferation of a glioma cell line and transfer Gaussia luciferase (Gluc) reporter activity to human brain microvascular endothelial cells (HBMVEC) (49).

In summary, tumor exosomes are capable of activating endothelial cells in a dose dependent manner, which may afford cancer a means of communicating with, manipulating, and "tuning" its host environment. It seems probable that a number of known cancer signaling pathways could be integrated in a compact exosomal vehicle, since the exosome is its self derived from the cancer cell but may escape immune surveillance and circulate in mass quantities. A future goal will be to design and construct novel approaches to intercept and manipulate this nanoscale cancer communication system for the purposes of understanding the mechanisms it may utilize to promote metastasis.

Supplementary Material

Refer to Web version on PubMed Central for supplementary material.

Acknowledgments

Financial Support: NIH U54 CA119342

References

1. Schorey JS, Bhatnagar S. Exosome Function: From Tumor Immunology to Pathogen Biology. Traffic. 2008; 9:871–881. [PubMed: 18331451]
2. Admyre C, Johansson SM, Paulie S, Gabrielsson S. Direct exosome stimulation of peripheral human T cells detected by ELISPOT. Eur J Immunol. 2006; 36:1772–1781. [PubMed: 16761310]
3. Lakkaraju A, Rodriguez-Boulan E. Itinerant exosomes: emerging roles in cell and tissue polarity. Trends Cell Biol. 2008; 18(5):199–209. [PubMed: 18396047]
4. Iero M, Valenti R, Huber V, Filipazzi P, Parmiani G, Fais S, et al. Tumour-released exosomes and their implications in cancer immunity. Cell Death Differ. 2008; 15(1):80–88. [PubMed: 17932500]
5. Taylor DD, Gercel-Taylor C. Tumour-derived exosomes and their role in cancer-associated T-cell signalling defects. British Journal of Cancer. 2005; 92:305–311. [PubMed: 15655551]
6. Liu C, Yu S, Zinn K, Wang J, Zhang L, Jia Y, et al. Murine Mammary Carcinoma Exosomes Promote Tumor Growth by Suppression of NK cell Function. The Journal of Immunology. 2006; 176:1375–1385. [PubMed: 16424164]
7. lero M, Valenti R, Huber V, Fillipazzi P, Parmiani G, Fais S, et al. Tumour-released exosomes and their implications in cancer immunity. Cell Death and Differentiation. 2008; 15:80–88. [PubMed: 17932500]
8. Bidard F-C, Pierga J-Y, Vincent-Salomon A, Poupon M-F. A "class action" against the microenvironment: do cancer cells cooperate in metastasis? Cancer Metastasis Rev. 2008; 27:5–10. [PubMed: 18066649]
9. Rinderknecht M, Detmar M. Tumor Lymphangiogenesis and Melanoma Metastasis. J Cell Physiol. 2008; 216:347–354. [PubMed: 18481261]
10. Mahabeleshwar GH, Byzova TV. Angiogenesis in Melanoma. Sem Onc. 2007; 34:555–565.
11. Thery C, Clayton A, Amigorena S, Raposo G. Isolation and Characterization of Exosomes from Cell Culture Supernatants and Biological Fluids. Current Protocols in Cell Biology. 2006; 3:22.21–23.22.29. [PubMed: 18228490]

12. Heijnen HF, Schiel AE, Fijnheer R, Geuze HJ, Sixma JJ. Activated platelets release two types of membrane vesicles: microvesicles by surface shedding and exosomes derived from exocytosis of multivesicular bodies and alpha-granules. Blood. 1999; 94(11):3791–3799. [PubMed: 10572093]

13. Raposo G, Nijman HW, Stoorvogel W, Liejendekker R, Harding CV, Melief CJ, et al. B lymphocytes secrete antigen-presenting vesicles. J Exp Med. 1996; 183(3):1161–1172. [PubMed: 8642258]

14. Winter PM, Neubauer AM, Caruthers SD, Harris TD, Robertson JD, Williams TA, et al. Endothelial αvβ3 Integrin-Targeted Fumagillin Nanoparticles Inhibit Angiogenesis in Atherosclerosis. Arterioscler Thromb Vasc Biol. 2006; 26:2103–2109. [PubMed: 16825592]

15. Winter PM, Schmieder AH, Caruthers SD, Keene JL, Zhang H, Wickline SA, et al. Minute dosages of αvβ3-targeted fumagillin nanoparticles impair Vx-2 tumor angiogensis and development in rabbits. FASEB J. 2008; 22:1–10. [PubMed: 18166582]

16. Haspel HC, Scicli GM, McMahon G, Scicli AG. Inhibition of Vascular Endothelial Growth Factor-Associated Tyrosine Kinase Activity with SU5416 Blocks Sprouting in the Microvascular Endothelial Cell Spheroid Model of Angiogenesis. Microvascular Research. 2002; 63:304–315. [PubMed: 11969307]

17. Stahl A, Wu X, Wenger A, Klagsbrun M, Kurschat P. Endothelial progenitor cell sprouting in spheroid cultures is resistant to inhibition by osteoblasts: A model for bone replacement grafts. FEBS Letters. 2005; 579:5338–5342. [PubMed: 16194535]

18. Walter-Yohrling J, Morgenbesser S, Rouleau C, Bagley R, Callahan M, Weber W, et al. Murine Endothelial Cell Lines as Models of Tumor Endothelial Cells. Clin Cancer Res. 2004; 10:2179–2189. [PubMed: 15041739]

19. Sin N, Meng L, Wang MQW, Wen JJ, Bornmann WG, Crews GM. The anti-angiogenic agent fumagillin covalently binds and inhibits the methionine aminopeptidase, MetAP-2. Proc Natl Acad Sci. 1997; 94:6099–6103. [PubMed: 9177176]

20. Thery C, Boussac M, Veron P, Ricciardi-Castagnoli P, Raposo G, Garin J, et al. Proteomic analysis of dendritic cell-derived exosomes: a secreted subcellular compartment distinct from apoptotic vesicles. J Immunol. 2001; 166(12):7309–7318. [PubMed: 11390481]

21. Wolfers J, Lozier A, Raposo G, Regnault A, Thery C, Masurier C, et al. Tumor-derived exosomes are a source of shared tumor rejection antigens for CTL cross-priming. Nat Med. 2001; 7(3):297–303. [PubMed: 11231627]

22. Riteau B, Faure F, Menier C, Viel S, Carosella ED, Amigorena S, et al. Exosomes bearing HLA-G are released by melanoma cells. Hum Immunol. 2003; 64(11):1064–1072. [PubMed: 14602237]

23. Mears R, Craven RA, Hanrahan S, Totty N, Upton C, Young SL, et al. Proteomic analysis fo melanoma-derived exosomes by two-dimensional polyacrylamide gel electrophoresis and mass spectrometry. Proteomics. 2004; 4:4019–4031. [PubMed: 15478216]

24. Sowinski S, Jolly C, Berninghausen O, Purbhoo MA, Chauveau A, Kohler K, et al. Membrane nanotubes physically connect T cells over long distances presenting a novel route for HIV-1 transmission. Nat Cell Biol. 2008; 10(2):211–219. [PubMed: 18193035]

25. Gurke S, Barroso JF, Hodneland E, Bukoreshtliev NV, Schlicker O, Gerdes H-H. Tunneling nanotube (TNT)-like structures facilitate a constitutive, actomyosin-dependent exchange of endocytic organelles between normal rat kidney cells. Exp Cell Res. 2008; 314:3669–3683. [PubMed: 18845141]

26. Rustom A, Saffrich R, Markovic I, Walther P, Gerdes H-H. Nanotubular Highways for Intercellular Organelle Transport. Science. 2004; 303(13):1007–1010. [PubMed: 14963329]

27. Brill A, Dashevsky O, Rivo J, Gozal Y, Varon D. Platelet-derived microparticles induce angiogenesis and stimulate post-ischemic revascularization. Cardiovasc Res. 2005; 67(1):30–38. [PubMed: 15878159]

28. Lazar-Molnar E, Hegyesi H, Toth S, Falus A. Autocrine and Paracrine Regulation by Cytokines and Growth Factors in Melanoma. Cytokine. 2000; 12(6)

29. Mahabeleshwar GH, Byzova TV. Angiogenesis in Melanoma. Semin Oncol. 2007; 34:555–565. [PubMed: 18083379]

30. Dirkx AEM, oude Egbrink MGA, Kuijpers MJE, van der Niet ST, Heijnen VVT, Bouma-ter Steege JCA, et al. Tumor Angiogenesis Modulates Leukocyte-Vessel Wall Interactions *in Vivo* by Reducing Endothelial Adhesion Molecule Expression. Caner Research. 2003; 63:2322–2329.

31. Chen LC, Laskin JD, Gordon MK, Laskin DL. Regulation of TREM expression in hepatic macrophages and endothelial cells during acute endotoxemia. Exp Mol Path. 2008; 84:145–155. [PubMed: 18222421]

32. Kaplan AP. Chemokines, Chemokine Receptors and Allergy. Int Arch Allergy Immunol. 2001; 124:423–431. [PubMed: 11340325]

33. Gu Y, Lewis DF, Groome LJ, Wang Y. Elevated Maternal IL-16 Levels, Enhanced IL-16 Expressions in Endothelium and Leukocytes, and Increased IL-16 Production by Placental Trophoblasts in Women with Preeclampsia. J Immunol. 2008; 181:4418–4422. [PubMed: 18768901]

34. Pap E, Pallinger E, Pasztoi M, Falus A. Highlights of a new type of intercellular communication: microvesicle-based information transfer. Inflamm Res. 2009; 58(1):1–8. [PubMed: 19132498]

35. Cocucci E, Racchetti G, Meldolesi J. Shedding microvesicles: artefacts no more. Trends Cell Biol. 2009; 19(2):43–51. [PubMed: 19144520]

36. Soleti R, Benameur T, Porro C, Panaro MA, Andriantsitohaina R, Martinez MC. Microparticles harboring Sonic Hedgehog promote angiogenesis through the upregulation of adhesion proteins and proangiogenic factors. Carcinogenesis. 2009; 30(4):580–588. [PubMed: 19168578]

37. Lynch SF, Ludlam CA. Plasma microparticles and vascular disorders. Br J Haematol. 2007; 137(1):36–48. [PubMed: 17359370]

38. Lechner D, Weltermann A. Circulating tissue factor-exposing microparticles. Thromb Res. 2008; 122 (Suppl 1):S47–54. [PubMed: 18691500]

39. Mostefai HA, Andriantsitohaina R, Martinez MC. Plasma membrane microparticles in angiogenesis: role in ischemic diseases and in cancer. Physiol Res. 2008; 57(3):311–320. [PubMed: 18597583]

40. Aharon A, Brenner B. Microparticles, thrombosis and cancer. Best Pract Res Clin Haematol. 2009; 22(1):61–69. [PubMed: 19285273]

41. Kim HK, Song KS, Chung JH, Lee KR, Lee SN. Platelet microparticles induce angiogenesis in vitro. Br J Haematol. 2004; 124(3):376–384. [PubMed: 14717787]

42. Leroyer AS, Rautou PE, Silvestre JS, Castier Y, Leseche G, Devue C, et al. CD40 ligand+ microparticles from human atherosclerotic plaques stimulate endothelial proliferation and angiogenesis a potential mechanism for intraplaque neovascularization. J Am Coll Cardiol. 2008; 52(16):1302–1311. [PubMed: 18929241]

43. Mezentsev A, Merks RM, O'Riordan E, Chen J, Mendelev N, Goligorsky MS, et al. Endothelial microparticles affect angiogenesis in vitro: role of oxidative stress. Am J Physiol Heart Circ Physiol. 2005; 289(3):H1106–1114. [PubMed: 15879485]

44. Yang C, Mwaikambo BR, Zhu T, Gagnon C, Lafleur J, Seshadri S, et al. Lymphocytic microparticles inhibit angiogenesis by stimulating oxidative stress and negatively regulating VEGF-induced pathways. Am J Physiol Regul Integr Comp Physiol. 2008; 294(2):R467–476. [PubMed: 18046016]

45. Janowska-Wieczorek A, Wysoczynski M, Kijowski J, Marquez-Curtis L, Machalinski B, Ratajczak J, et al. Microvesicles derived from activated platelets induce metastasis and angiogenesis in lung cancer. Int J Cancer. 2005; 113(5):752–760. [PubMed: 15499615]

46. Kim CW, Lee HM, Lee TH, Kang C, Kleinman HK, Gho YS. Extracellular membrane vesicles from tumor cells promote angiogenesis via sphingomyelin. Cancer Res. 2002; 62(21):6312–6317. [PubMed: 12414662]

47. Millimaggi D, Mari M, D'Ascenzo S, Carosa E, Jannini EA, Zucker S, et al. Tumor vesicle-associated CD147 modulates the angiogenic capability of endothelial cells. Neoplasia. 2007; 9(4): 349–357. [PubMed: 17460779]

48. Taraboletti G, D'Ascenzo S, Giusti I, Marchetti D, Borsotti P, Millimaggi D, et al. Bioavailability of VEGF in tumor-shed vesicles depends on vesicle burst induced by acidic pH. Neoplasia. 2006; 8(2):96–103. [PubMed: 16611402]

49. Skog J, Wurdinger T, van Rijn S, Meijer DH, Gainche L, Sena-Esteves M, et al. Glioblastoma microvesicles transport RNA and proteins that promote tumour growth and provide diagnostic biomarkers. Nat Cell Biol. 2008; 10(12):1470–1476. [PubMed: 19011622]
50. Al-Nedawi K, Meehan B, Micallef J, Lhotak V, May L, Guha A, et al. Intercellular transfer of the oncogenic receptor EGFRvIII by microvesicles derived from tumour cells. Nat Cell Biol. 2008; 10(5):619–624. [PubMed: 18425114]
51. Gesierich S, Berezovskiy I, Ryschich E, Zoller M. Systemic induction of the angiogenesis switch by the tetraspanin D6. 1A/CO-029. Cancer Res. 2006; 66(14):7083–7094. [PubMed: 16849554]
52. Hanahan D, Folkman J. Patterns and Emerging Mechanisms of the Angiogenic Switch during Tumorigenesis. Cell. 1996; 86:353–364. [PubMed: 8756718]
53. Valenti R, Huber V, Iero M, Filipazzi P, Parmiani G, Rivoltini L. Tumor-Released Microvesicles as Vehicles of Immunosuppression. Cancer Research. 2007; 67(7):2912–2915. [PubMed: 17409393]
54. Bin KJ. Three-dimensional tissue culture models in cancer biology. Seminars in Cancer Biology. 2005; 15:365–377. [PubMed: 15975824]
55. Valster A, Tran NL, Nakada M, Berens ME, Chan AY, Symons M. Cell migration and invasion assays. Methods. 2005; 37:208–215. [PubMed: 16288884]
56. Yamada KM, Cukierman E. Modeling Tissue Morphogenesis and Cancer in 3D. Cell. 2007; 130:601–610. [PubMed: 17719539]
57. Zhou Q, Kiosses WB, Liu J, Schimmel P. Tumor endothelial cell tube formation model for determining anti-angiogenic activity of a tRNA synthetase cytokine. Methods. 2008; 44:190–195. [PubMed: 18241800]
58. Sun X-T, Zhang M-Y, Shu C, Li Q, Yan X-G, Cheng N, et al. Differential gene expression during capillary morphogenesis in a microcarrier-basedthree-dimensional *in vitro* model of angiogenesis with focus on chemokines and chemokine receptors. World J Gastroenterol. 2005; 11(15):2283–2290. [PubMed: 15818740]
59. Taylor DD, Gercel-Taylor C. MicroRNA signatures of tumor-derived exosomes as diagnositic biomarkers of ovarian cancer. Gynecol Onc. 2008; 110:13–21.

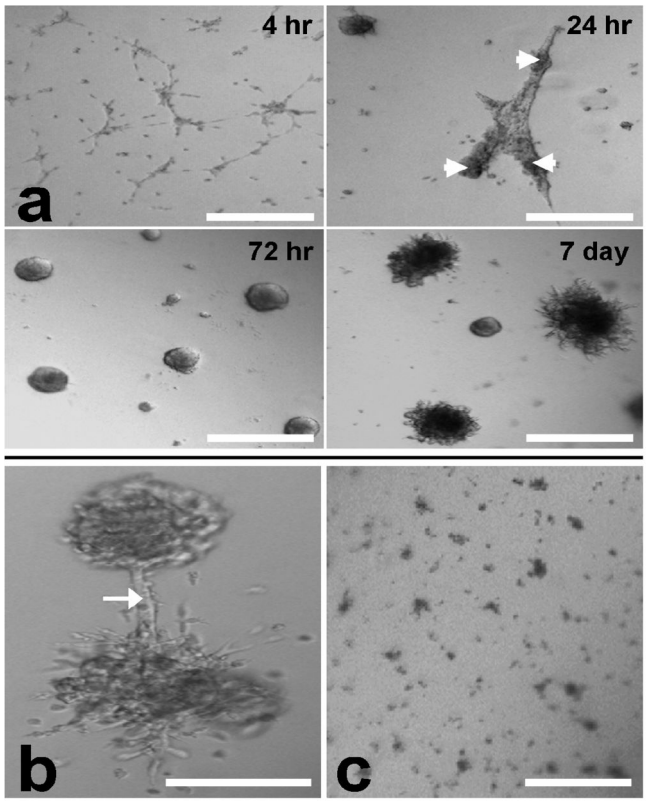

Figure 1.
2F-2B endothelial cells (50,000/well) spontaneously form spheroids on 3D matrigel as evidenced by phase contrast microscopy. (**a**) cells migrate into a lace-like network by 4 hrs. Endothelial tubules form and begin contracting into spheroids (arrowheads) by 24hrs. Formation of spheroids occurs following 72 hrs in culture. Circumferential spheroid sprouting is observed by 7 days. (**b**) Beyond 7 day culture, spheroids sprouts can form anastomotic connections (arrow). (**c**) In the presence of anti-angiogenic fumagillin nanoparticles for 72 hrs (final culture fumagillin concentration = 4 μM) spheroids fail to develop. Bar = 200 μm.

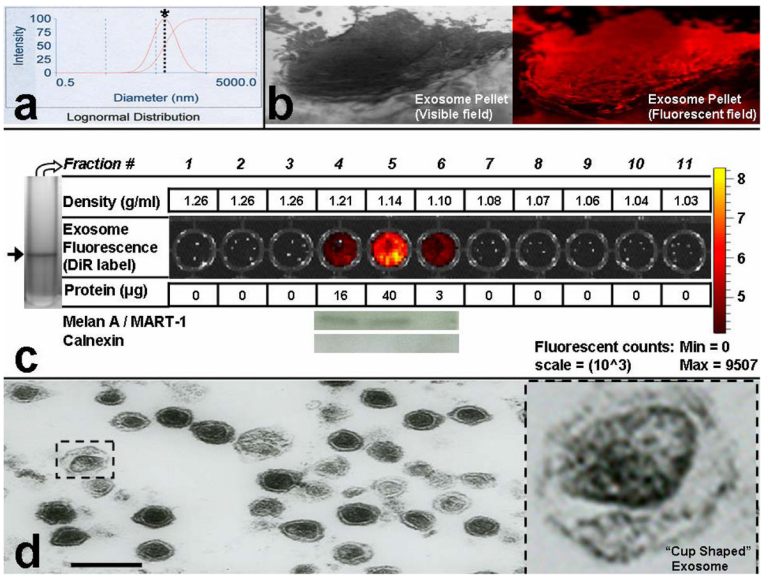

Figure 2.

Isolation of B16-F10 melanoma exosomes. (**a**) Dynamic light scattering (DLS, Brookhaven Instruments Corp.) was used to confirm exosome isolation and size exosomes (prior to centrifugation at 100,000 × g to maximize accuracy by minimizing the measurement of exosome clusters). Exosome size distribution profile = bell shaped curve. Dotted line crosses the logarithmic sizing curve at * = 74 nm (s.dev. =13 nm, average of 24 individual measurements). (**b**) Exosome pellet visualized through a 70 Ti polycarbonate tube following differential centrifugation; 20 X magnification. Exosomes were treated with DiI prior to pellet formation and display red fluorescence via fluorescent microscopy; 20 X magnification. (**c**) DiR labeled B16 melanoma exosome flotation on a continuous sucrose gradient (2.0 – 0.25 M). Arrow = single blue exosome band (black and white image, DiR is blue in visible light wavelengths) band present in gradient fraction 5 of the SW 41 centrifuge tube. Exosome fractions were further evaluated for protein content and expression of Melan A or Calnexin marker proteins. (**d**) Transmission electron microscopy was used to confirm isolation of cup shaped (see blow up) B16 melanoma exosomes. Various exosome sizes ~50–100 nm are observed in concordance with DLS. Black scale bar = 200 nm.

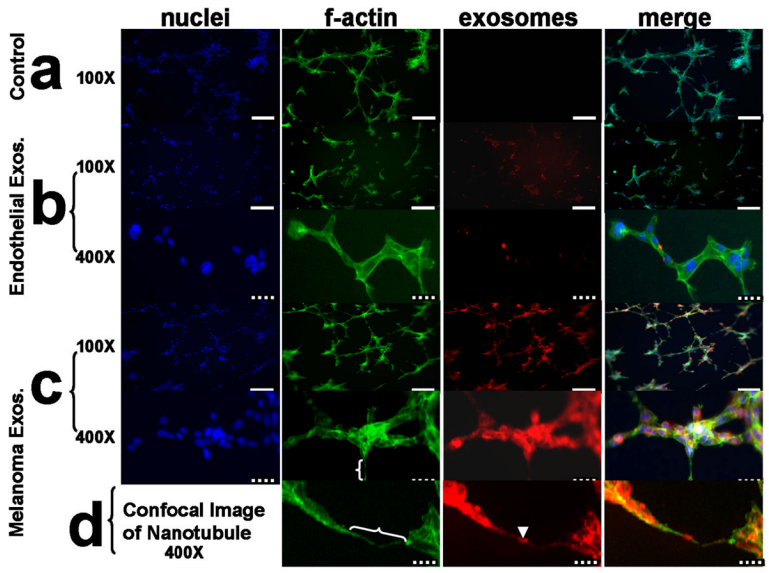

Figure 3.

Exosomes interact with and influence the morphology of 3D 2F-2B endothelial cell tubules as evidenced by fluorescent microscopy. (**a**) 2F-2B endothelial cells (100,000/chamber) cultured on matrigel for 24 hrs in the absence of exogenously labeled exosomes show no red background signal while f-actin is stained green. (**b**) endothelial cells (100,000/chamber) cultured on matrigel for 24 hrs in the presence of 20 μg/ml of 2F-2B endothelial cell exosomes demonstrate decreased tubule branching versus (a) and show exosome signal in red clusters within green f-actin stained endothelial tubules. (**c**) endothelial cells (100,000/chamber) cultured on matrigel for 24 hrs in the presence of 20 μg/ml of B16 melanoma exosomes demonstrate increased tubule branching versus (a) and show colocalization between exosome signal in red clusters and green f-actin stained endothelial tubules. (**d**) Confocal image of red exosome signal co-localized with green stained f-actin in a nanotube bridging two endothelial tubules. white brackets = nanotubes; arrowhead = exosome cluster within a nanotube; solid white bar = 200 μm; hatched bar = 40 μm. Blue fluorescence = DAPI (Vector labs), green = AlexaFluor 488 phalloidin (invitrogen), red = DiI (invitrogen).

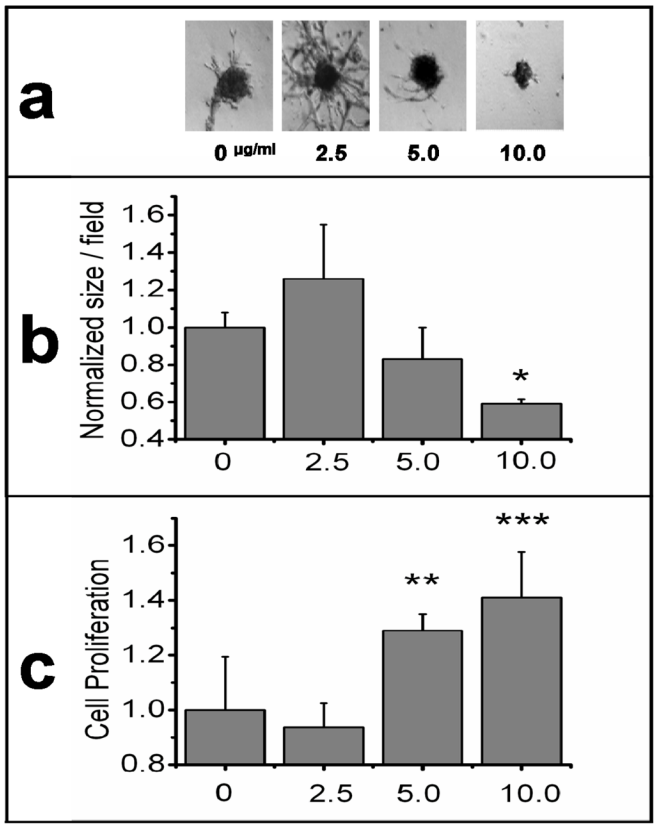

Figure 4.

Long Term Effects of varying B16-F10 melanoma exosome concentrations on 3D endothelial culture. 2F-2B endothelial cells (50,000/well) were cultured for 72 hrs to form spheroids followed by the addition of 0, 2.5, 5, or 10 µg/ml for 10 days to study the permanence of exosome effects on spheroid development. (**a**) phase contrast microscopy of representative spheroid morphology for each exosome dose. (**b**) ImageJ software was used to measure the area of individual spheroids in 40 X mag. fields (see supplemental information, Fig. S1). Average spheroid size/field was normalized against control (0 µg). ANOVA was used to calculate significance for $p < 0.05$ for a control of N = 48; * = p = 5.4×10^−5. Error bars represent the standard deviation of the average spheroid size from 3 random fields from different cultures. (**c**) XTT (tetrazolium salt) colorimetric reagent (MD Biosciences; St. Paul MN) was used to measure cell proliferation. Average endothelial cell proliferation was normalized against control (0 µg exosomes). ANOVA was used to calculate significance for $p < 0.05$ for a control of N = 4; ** = p = 5.9×10^−3 and *** = p = 2.9×10^−3. Error bars represent the standard deviation of N = 4 samples.

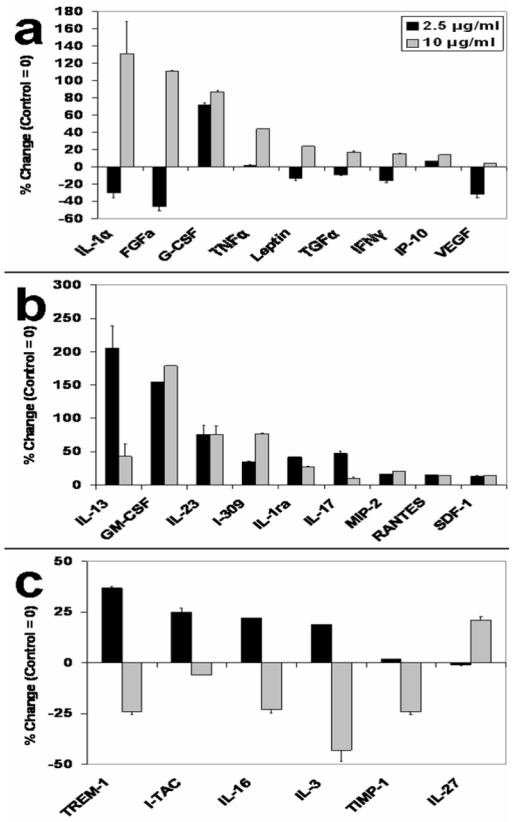

Figure 5.

Melanoma exosomes modulate endothelial cytokine production. 2F-2B endothelial cells (50,000/well) were cultured for 72 hrs to form spheroids followed by the addition of 0, 2.5, or 10 μg/ml for 10 days to produce cytokines in the spheroid culture media. Three sets of culture media samples were collected and pooled for each exosome dosing group and analyzed using cytokine arrays. (**a**) TransSignal Mouse Angiogenesis Antibody Array (Panomics) or (**b, c**) Proteome Profiler Mouse Cytokine Array (R&D Systems). Cytokines levels are represented as a percent change over control (control = 0). The absolute change in level for each cytokine group (2.5 and 10 μg/ml melanoma exosomes) was averaged. The average of absolute changes for all cytokines was 41%. ANOVA analysis was used to calculate statistical significance. Cytokine levels that changed more than 10% from the absolute value average changes as compared to a normalized control group were considered to be affected by the experimental procedures, according to ANOVA that revealed statistical significance ($p < 0.05$) for difference from control in each case. The p values for 2.5, 10 and combined are 0.035, 0.016 and 0.001 respectively. Error bars = s.e.m. of replicates present on the arrays.